

Rigid Restraint Thermal Self-Compressing Bonding of Ti6Al4V Alloy by Local Induction Heating

Pan Rui¹, Deng Yunhua², Zhang Hua¹

¹ School of Mechanical Engineering, Beijing Institute of Petrochemical Technology, Beijing 102600, China; ² Aeronautical Key Laboratory for Welding and Joining Technologies, AVIC Manufacturing Technology Institute, Beijing 100024, China

Abstract: Rigid restraint thermal self-compressing bonding (TSCB) by local induction heating is a new diffusion bonding technique proposed in this research. Experiments were conducted on Ti6Al4V plates to prove the feasibility of rigid restraint thermal self-compressing bonding by local induction heating. Moreover, finite element analysis was employed to numerically investigate the thermal elastic-plastic stress-strain cycle during thermal self-compressing bonding by local induction heating. Results show that the solid-state joint has homogeneous microstructure and excellent mechanical properties. By local induction heating, an internal elasto-plastic stress-strain field is developed which makes the bond interface subjected to thermal compressive action. This thermal self-compressing action combined with the high temperature on the bond interface promotes the atom diffusion across the bond interface to produce solid-state joints.

Key words: local induction heating; rigid restraint thermal self-compressing bonding; thermal stress-strain evolution; finite element analysis

With the rapid development of aerospace industry, the demand for materials with high performance is increasing. Titanium alloy has the characteristics of low density, high specific strength, excellent low temperature performance and excellent corrosion resistance, so it is widely employed in the aeronautical industry. The proportion of high-performance titanium alloy usage has even become an important indicator to estimate the development of aerospace industry. The manufacturing of titanium alloys inevitably requires the use of welding^[1-8]. Usually, titanium alloy welding methods include fusion welding (electron beam welding, tungsten argon arc welding, plasma arc welding, and laser welding), brazing, and solid phase welding (friction stir welding, diffusion welding). In comparison with other welding methods, the materials to be joined do not melt during diffusion bonding. Welding in a vacuum ensures that the surface of the material is not contaminated or oxidized and defects such as incomplete penetration, porosity, oxide inclusions, and other disadvantages will not exist^[9-16]. However, conventional vacuum diffu-

sion bonding has disadvantages such as long bonding time and external forces. Based on conventional vacuum diffusion bonding, our team^[17,18] proposed a new type of diffusion bonding method-thermal self-compressing bonding (TSCB) by electron beam heating. Experiments were performed on Ti6Al4V titanium alloy plates with thickness of 5 mm. Joints with microstructures similar to those of the base metal were obtained. However, it is found that the temperature gradient along the plate thickness direction is large due to single surface heating by electron beam. Thus the bottom surface temperature is relatively low, resulting in an inverse effect of bonding rate. At the same time, due to the limitation of the electron gun magnetic deflection coil, the heating range by electron beam is restricted. Induction heating uses an alternating magnetic field to generate an induced current which generates resistance heat^[19,20]. Compared with concentrated heat sources, such as electron beam heating, temperature gradient along the plate thickness direction during induction heating is more uniform. In order to avoid the

Received date: February 04, 2020

Foundation item: National Natural Science Foundation of China (51705491)

Corresponding author: Zhang Hua, Ph. D., Professor, School of Mechanical Engineering, Beijing Institute of Petrochemical Technology, Beijing 102600, P. R. China, Tel: 0086-10-81292220, E-mail: huazhang@bipt.edu.cn

Copyright © 2021, Northwest Institute for Nonferrous Metal Research. Published by Science Press. All rights reserved.

temperature gradient along the plate thickness direction by electron beam, induction heating was employed in this work. The schematic of TSCB by local induction heating is shown in Fig.1.

The fundamental principle is to produce a thermal elastic-plastic stress-strain field which compresses the high temperature thermoplastic metal at the bonding surface by local induction heating. The thermal elastic-plastic stress-strain field is achieved by local induction heating through the rigidly constrained zones. Thus atom diffusion across the bonding interface occurs. Because of the high temperature and pressure, atomic diffusion across the interface is facilitated and solid-state bonding is achieved. Experiments were conducted on Ti6Al4V plates to prove the feasibility of TSCB by local induction heating. Moreover, in order to investigate the bonding mechanism and bonding characteristic of TSCB by induction heating, on the basis of experiment process, thermal stress-strain evolution finite element analysis model during bonding was established.

1 Experiment

Ti6Al4V titanium plates with the thickness of 5 mm were cut to 60 mm (L) \times 50 mm (W) \times 5 mm (H). Microstructure of base metal consists of equiaxed α structures and intergranular β structures, as shown in Fig.2.

To facilitate diffusion bonding, surface of specimens to be bonded was grinded to a roughness of $R_a=0.8$ and pickled to

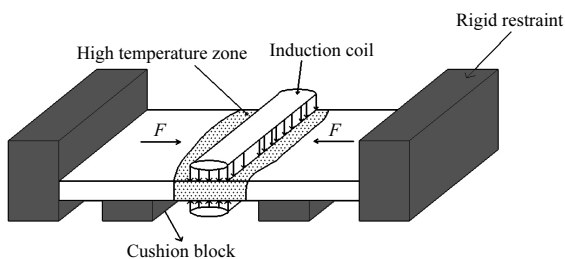


Fig.1 Schematic diagram of TSCB by local induction heating

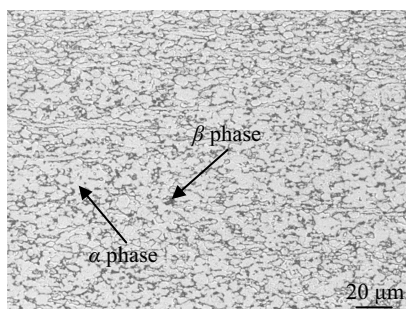


Fig.2 Microstructure of base metal

remove the surface oxides, oils and other contaminants. The specimens after preparation were assembled, as shown in Fig.1.

The Ti6Al4V titanium alloy specimens to be bonded were locally heated by an induction heating device, and an infrared camera device was used for temperature control. The experiment parameters are illustrated in Table 1.

After TSCB by local induction heating, the specimens for metallographic analysis were machined through the bonding interface and the cross-section samples were grinded and polished. Three tensile specimens of joints and base metals were respectively machined. Tensile specimens were tested by mechanical property testing machine.

2 Results

2.1 Microstructure of bonded joint

The microstructure of the joint is shown in Fig.3. The bonding interface almost disappears. Microstructure of bonded area consists of equiaxed α structures and intergranular β structures which is similar to that of base metal. This is because the peak temperature of the heating zone during bonding is 950 °C which is lower than the $\beta \rightarrow \alpha$ phase transition temperature of the Ti6Al4V titanium alloy (997 ± 15 °C).

2.2 Mechanical properties of bonded joint

Mechanical properties of Ti6Al4V TSCB joints by local induction heating and Ti6Al4V base metals are shown in Table 2. The average values of tensile strength, yield strength and elongation of base metal are 1069.81 MPa, 1042.88 MPa and 16.05%, respectively and those of the joint are 995.7 MPa, 912.7 MPa and 14.15%, respectively. The mechanical properties of the joint are close to those of base metal, which shows that the experiment obtains a joint with good mechanical properties.

3 Finite Element Analysis of Thermal Stress-Strain Evolution

In order to investigate the bonding mechanism and bonding

Table 1 Experiment parameters

Current/A	Holding temperature/°C	Holding time/min
680	950	7.5

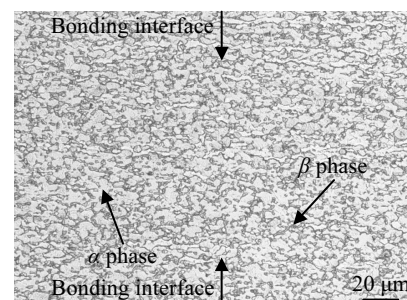


Fig.3 Microstructure of TSCB joint by local induction heating

Table 2 Mechanical properties of joints and base metals

Property	Tensile strength/ MPa	Average tensile strength/MPa	Yield strength/ MPa	Average yield strength/MPa	Elongation/ %	Average elongation/ %
Base metal	1064.83		1033.14		16.96	
	1078.75	1069.81	1056.94	1042.88	16.04	16.05
	1065.85		1038.55		15.16	
Joint	1001		922		13.36	
	994	995.7	906	912.7	15.04	14.15
	992		910		14.04	

characteristic of TSCB, based on experiment process, thermal stress-strain evolution finite element analysis model during bonding was established.

According to the experiments, a finite element model by local induction heating was established using Ansys software. As shown in Fig.4, the mesh size near the interface is 1 mm×1 mm×1 mm, and the mesh size away from the interface is 2.5 mm×2.5 mm×2.5 mm.

The material used in the experiment is TC4 titanium alloy with a density of 4430 kg·m⁻³ and Poisson's ratio of 0.34. Other related material parameters are shown in Table 3 and Table 4.

3.1 Electromagnetic analysis

Induction heating uses an alternating magnetic field to generate induced current which generates resistance heat. A three-dimensional model is built by Maxwell software, which considers the eddy current effect and the skin effect to solve the current density field. Since the current changes with time during the actual experiment, two currents are used in the calculation to simulate the actual current change. The parameters used in the calculation are shown in Table 5.

3.2 Thermal and static analysis

The calculated current density field is imported to the Ansys transient thermal analysis module to calculate the heat flux field. Set the heating time as 70 s, holding time as 450 s, cooling time as 600 s and calculate the transient temperature field.

The thermal parameters are based on the common range of Ti6Al4V temperature field simulation^[21,22] and adjusted

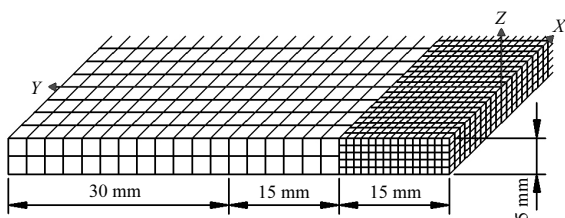


Fig.4 Geometry model and mesh generation

Table 3 Temperature-dependent thermophysical properties of Ti6Al4V titanium alloy^[18]

Temperature/ °C	Thermal con- ductivity/W·m ⁻¹ ·K ⁻¹	Specific heat/ J·kg ⁻¹ ·K ⁻¹	Thermal expansion coefficient/×10 ⁻⁶ K ⁻¹
20	6.8	611	9.1
100	7.4	624	9.2
200	8.7	653	9.3
300	9.8	674	9.5
400	10.3	691	9.7
500	11.8	703	10

Table 4 Temperature-dependent thermomechanical properties of Ti6Al4V titanium alloy^[18]

Temperature/ °C	Resistivity/ μΩ·m	Young's modulus/GPa	Yield strength/MPa	Tangent modulus/GPa
20	1.7	-	920	3.77
22	-	113.2	-	-
100	1.76	-	-	-
150	-	98	-	-
200	1.82	-	750	2.73
250	-	90	-	-
300	1.86	-	-	-
350	-	83	-	-
400	1.89	-	560	2.09
450	-	75	-	-
500	1.91	-	-	-
550	1.92	-	-	-
600	1.92	61	340	1.76
700	1.92	50	280	-
800	1.91	40	130	0.125
900	-	35	-	-
1000	-	25	90	-
1200	-	20	66	-

Table 5 Electromagnetic parameters

Current/A	Current frequency/kHz
750	46.2
810	46.2

according to the real temperature field data in the calculation process. The thermal parameters are shown in Table 6.

The calculated transient temperature field is imported to the Ansys static analysis module. Fix the clamp supports at both ends and only allow the lateral displacement, and then calculate the stress and strain field.

3.3 Verification of the finite element model

In order to verify the finite element model, temperature at center points of the upper surface of the joint region and the residual stress distribution were measured. The upper surface center point temperature was measured by infrared camera in real time. The temperature at the points 10 and 20 mm away from the center point of the bonding interface was measured by B type thermocouple with the diameter of 0.5 mm. The temperature recorder is Yokogawa temperature multi-channel paperless recorder. The residual stress was measured by X-ray diffraction method. The target material is Cu and the diffraction plane is (213). The X-ray residual stress was measured by the testing center of AVIC Manufacturing Technology Institute.

In comparison with the simulation results, the measured results are in good agreement with the simulation results, which proves the accuracy of the finite element model, as shown in Fig.5 and Fig.6.

3.4 Thermal cycle and temperature distribution during TSCB by local induction heating

The calculated thermal cycles at center points of the bonding interface are shown in Fig.7. The difference between maximum temperature and minimum temperature along thickness direction is less than 3 °C while the temperature difference is about 110 °C with local heating by electron beam^[17,18]. Compared with local heating by electron beam, the temperature field distribution of TSCB by induction heating is uniform along the thickness direction.

The highest temperature at the bond interface is about 952 °C, which is lower than the $\beta \rightarrow \alpha$ phase transition temperature of the Ti6Al4V titanium alloy (997 ± 15 °C), so uniform microstructure after bonding (Fig.3) and good mechanical properties (Table 2) are obtained.

The temperature distribution of the upper surface after

Table 6 Thermal parameters

Thermal parameter	Value
Thermal emissivity	0.7
Surface heat transfer coefficient/ $W \cdot m^{-2} \cdot ^\circ C^{-1}$	20
Surface heat convection coefficient/ $W \cdot m^{-2} \cdot ^\circ C^{-1}$	50

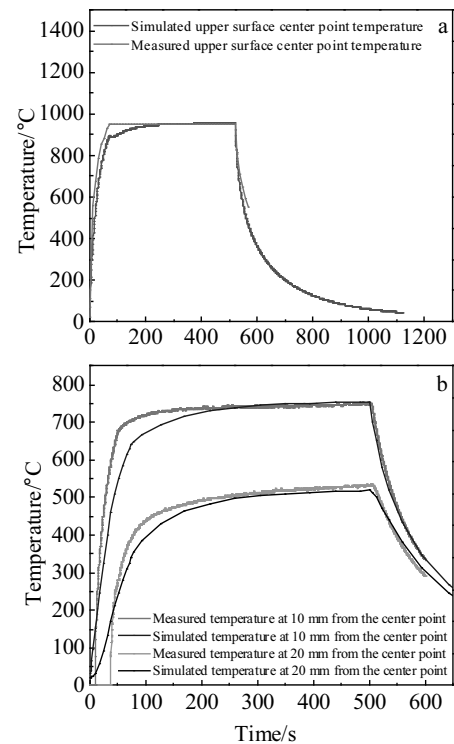


Fig.5 Comparison of simulated and measured temperature at different points: (a) surface center point and (b) 10 and 20 mm away from the center point

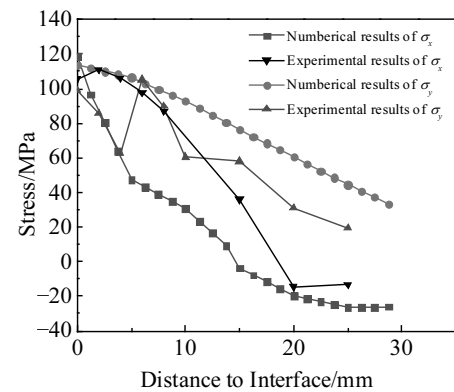


Fig.6 Comparison of simulated and measured residual stress

heating is shown in Fig.8. It can be seen that there is a significant temperature gradient perpendicular to the direction of the joint interface: the temperature at the interface is the highest and it gradually descends away from the interface.

3.5 Thermal stress-strain evolution during TSCB by local induction heating

The thermal stress-strain evolution at the center point of bond interface is shown in Fig.9. The results show that the transverse stress and the longitudinal stress at the center point

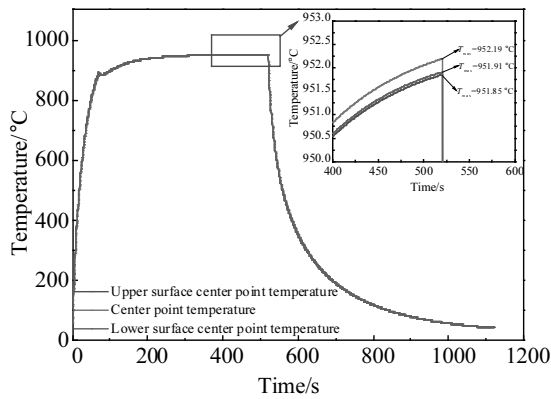


Fig.7 Thermal cycles of center points

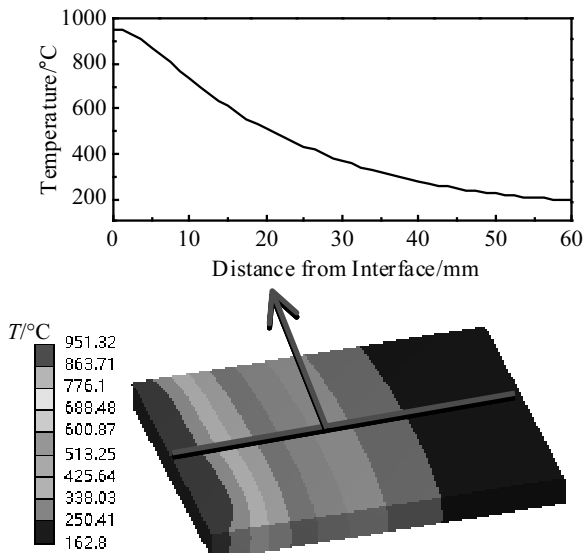


Fig.8 Temperature distribution of the upper surface after heating

are compressive stress during the heating process. The main reason is that during local heating, materials at the interface area with high temperature expand, but the surrounding cold metal restrains the expansion of materials and the compressive stress occurs at the bond interface.

As shown in Fig.9a, the transverse stress and longitudinal stress increase with time. At the moment of $t=60$ s, the transverse compressive stress comes to a peak value of -250 MPa, which is larger than the yield strength of the Ti6Al4V titanium alloy. So the material plastically deforms, as shown in Fig.9b. Subsequently, the yield strength of the material gradually decreases with the increase of temperature, so the transverse compressive stress and the longitudinal compressive stress gradually decrease.

The transverse compressive stress at the end of heating

period comes to -120 MPa. During the heat preservation process, the temperature and stress value are almost unchanged. During the cooling process, the metal at the interface zone shrinks as the temperature gradually decreases. However, since the shrinkage is restricted by the surrounding cold metal, the compressive stress gradually transforms to the tensile stress. Finally when the temperature reaches to room temperature, the residual tensile stress produces.

During the diffusion bonding process, the cross-sectional temperature and the related lateral stress distribution are shown in Table 7. As the heating time prolongs, the temperature at the interface gradually increases, and at the same time, the interface is subjected to the transverse compressive stress, resulting in significant plastic deformation. It can be seen from the simulation results that by local induction heating, an internal elasto-plastic stress-strain field is developed which makes the bond interface subjected to thermal compressive action according to the finite element analysis. This thermal self-compressing action combined with high temperature on the bond interface promotes the atom diffusion across the bond interface to produce solid-state bonding.

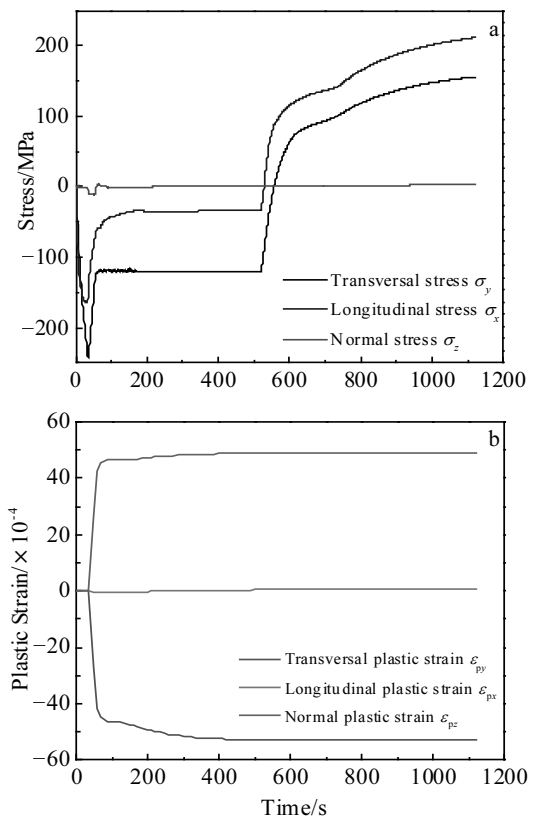
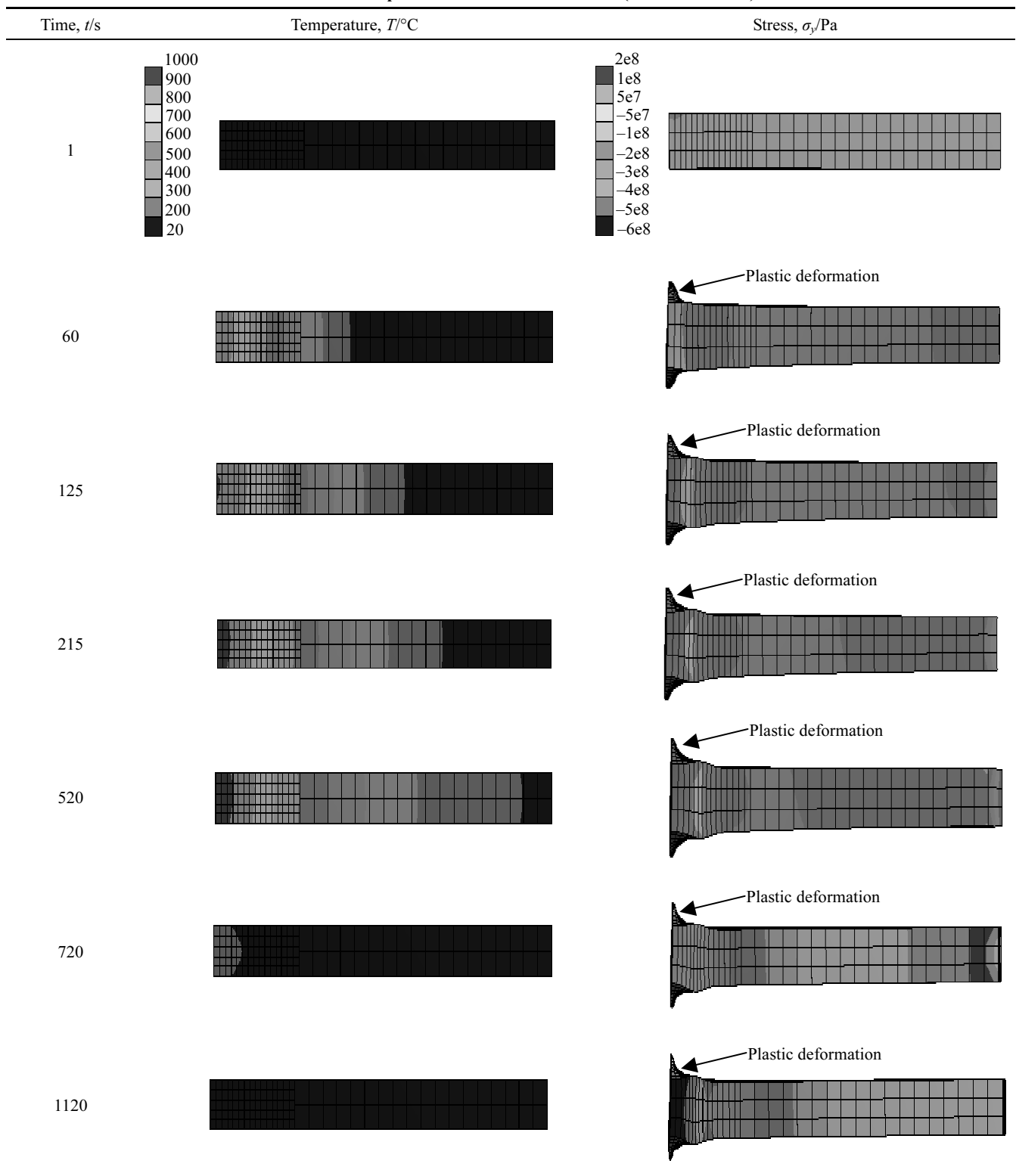


Fig.9 Thermal stress (a) and plastic strain (b) evolution at the center point of bond interface during bonding

Table 7 Center cross-section temperature and stress distribution (deformation $\times 20$) at different times

4 Conclusions

1) Ti6Al4V plates can be joined through rigid restraint thermal self-compressing bonding by local induction heating. Solid-state joint with great bond quality can be attained.

2) Microstructure of Ti6Al4V bonded area consists of

equiaxed α structures and intergranular β structures which is similar to that of the base metal. The average values of tensile strength, yield strength and elongation of the joint are 995.7 MPa, 912.7 MPa and 14.15%, respectively, which are approximately equivalent to those of the base metal.

3) By local induction heating, an internal elasto-plastic

stress-strain field is developed which makes the bond interface subjected to thermal compressive action according to the finite element analysis. This thermal self-compressing action combined with high temperature on the bond interface promotes the atom diffusion across the bond interface to produce solid-state joints during rigid restraint thermal self-compressing bonding by local induction heating.

References

- Arrieta J, Striz A J. *Structural and Multidisciplinary Optimization*[J], 2005, 30(2): 155
- Wang Xiangming, Liu Weiyan. *Design and Application of Titanium Alloy Structure for Aircraft*[M]. Beijing: National Defense Industry Press, 2010 (in Chinese)
- Huda Z, Edi P. *Materials & Design*[J], 2013, 46: 552
- Williams J C, Starke E A. *Acta Materialia*[J], 2003, 51(19): 5775
- Soutis C. *Progress in Aerospace Sciences*[J], 2005, 41(2): 143
- Huda Z, Zaharinie T, Min G J. *Journal of Aerospace Engineering*[J], 2010, 23(2): 124
- Fang Lianjun, Kan Tiantian, Tan Weilong. *New Technology New Products of China*[J], 2014(11): 92 (in Chinese)
- Gao Wenjing, Lei Junxiang. *Nonferrous Metal Materials and Engineering*[J], 2017, 38(4): 239 (in Chinese)
- Huang J L, Warnken N, Gebelin J C. *Acta Materialia*[J], 2012, 60(6-7): 3215
- Wu Huiqiang, Feng Jicai, He Jingshan et al. *Transaction of the China Welding Institution*[J], 2004, 25(4): 59 (in Chinese)
- Liu J, Gao X L, Zhang L J et al. *Journal of Materials Engineering and Performance*[J], 2015, 24(1): 319
- Liu H J, Feng X L. *Rare Metal Materials and Engineering*[J], 2009, 38(9): 1509
- Cam G, Kocak M. *Science and Technology of Welding and Joining*[J], 1998, 3(3): 105
- Han Xiufeng, Zhang Lu, Qian Linyi. *Aeronautical Manufacturing Technology*[J], 2012, 409(13): 55 (in Chinese)
- Kurt B, Orhan N, Evin E et al. *Materials Letters*[J], 2007, 61(8-9): 1747
- Wang X R, Yang Y Q, Luo X. *Intermetallics*[J], 2013, 36: 127
- Deng Yunhua, Guan Qiao, Wu Bing et al. *Materials Letters*[J], 2014, 129: 43
- Deng Yunhua, Guan Qiao, Tao Jun et al. *Chinese Journal of Mechanical Engineering*[J], 2018, 31(1): 1
- Sun Ning. *Metal Processing*[J], 2010(24): 47 (in Chinese)
- Wang Juan, Liu Qiang. *Brazing and Diffusion Welding Technology*[M]. Beijing: Chemical Industry Press, 2012 (in Chinese)
- Wen Quan. *Finite Element Simulation and Formability of Friction Stir Welded TC4 Titanium Alloy Lap Joints*[D]. Shenyang: Shenyang Aerospace University, 2016 (in Chinese)
- Li Wei. *Numerical Simulation of Inertial Friction Welding Process of TC4 Titanium Alloy*[D]. Changchun: Changchun University of Technology, 2018 (in Chinese)

TC4 钛合金局部感应加热刚性拘束热自压扩散连接与机理分析

潘睿¹, 邓云华², 张华¹

(1. 北京石油化工学院 机械工程学院, 北京 102600)

(2. 中国航空制造技术研究院 航空焊接与连接技术航空科技重点实验室, 北京 100024)

摘要: 提出了一种新型扩散连接方法——局部感应加热刚性拘束热自压扩散 (TSCB)。利用 TC4 板材进行了实验, 验证了局部感应加热刚性拘束热自压扩散方法的可行性。在实验基础上建立了感应加热刚性拘束热自压扩散过程热应力应变有限元分析模型, 揭示了钛合金局部感应加热刚性拘束热自压扩散连接机理。实验结果表明, 感应加热刚性拘束热自压扩散原理合理, 接头显微组织均匀, 综合力学性能较好。热应力应变过程有限元数值分析表明, 在刚性拘束的待连接材料对接区域进行局部感应加热时, 界面附近形成热拘束应力应变场, 对界面处高温热塑性状态金属进行热挤压, 促进界面两侧原子扩散, 最终实现了固相连接。

关键词: 局部感应加热; 热自压扩散连接; 热应力应变过程; 有限元分析

作者简介: 潘睿, 男, 1995 年生, 硕士, 北京石油化工学院机械工程学院, 北京 102600, E-mail: panrui008@163.com